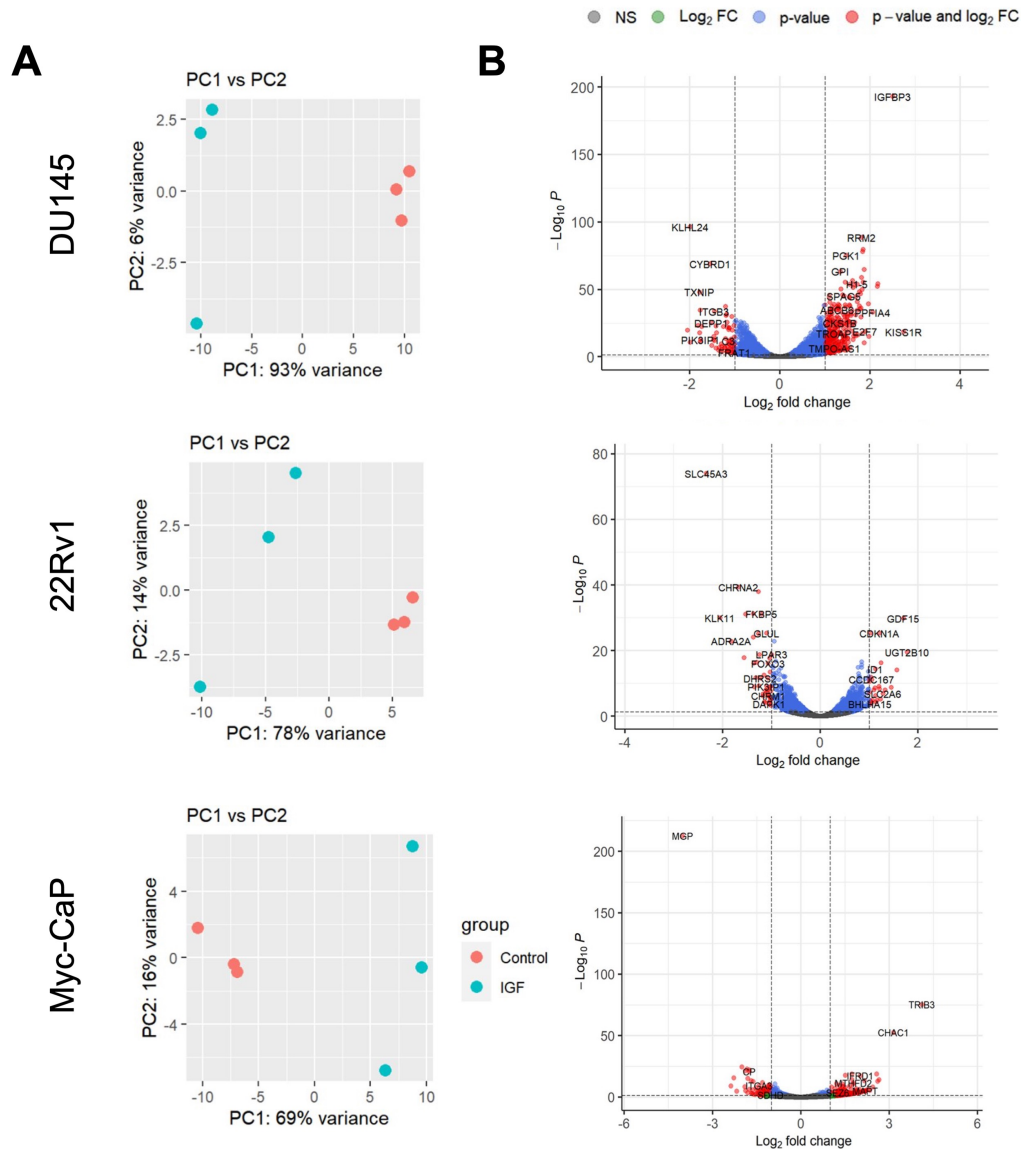
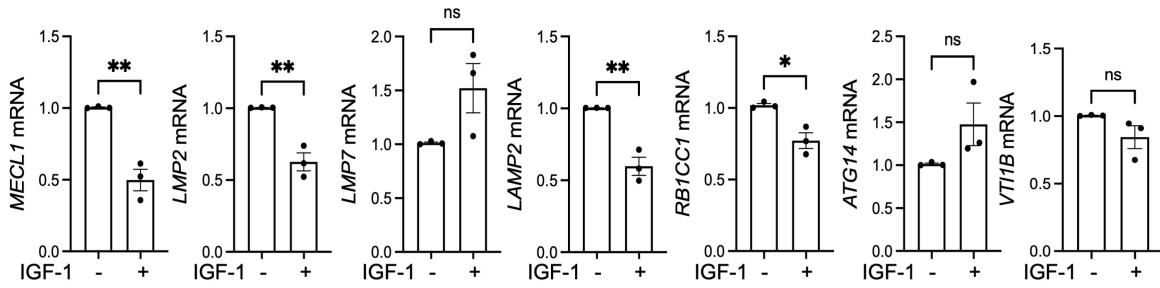


Nandakumar et al Supplementary Figures

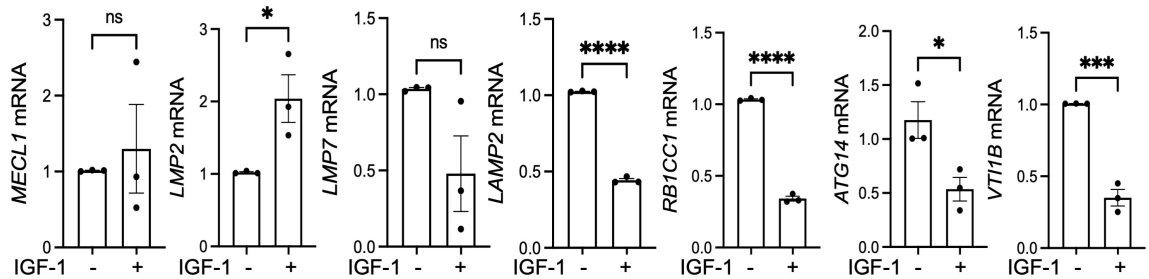


Supplementary Figure S1. Effect of IGF-1 on transcriptome of PCa cells. DU145, 22Rv1 and Myc-CaP cells were serum starved for 24 hrs, treated with 30 nM IGF-1 or solvent (control) for 24 hrs and RNA was extracted for sequencing. **A.** Principal component analysis (PCA) of RNA sequencing data (top 500 genes) for the three cell lines displaying the variation of each sample with respect to their transcriptomic profile. The x-axis shows the first principal component (PC1), accounting for the largest amount of variation in the experiment and the y-axis shows the second principal component (PC2). **B.** Volcano plots displaying the top high and low differentially expressed genes.

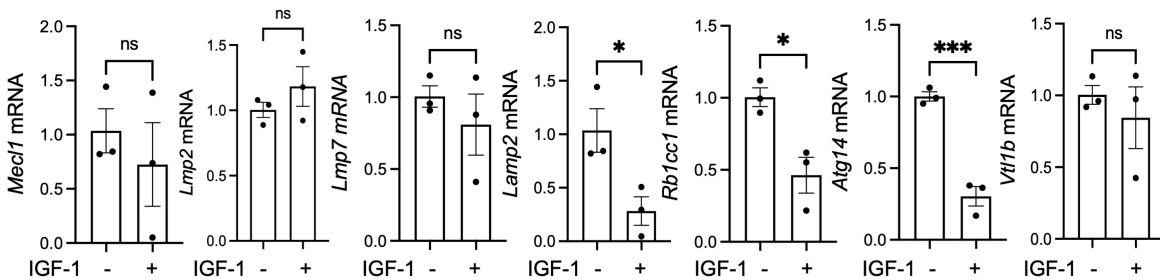
A DU145



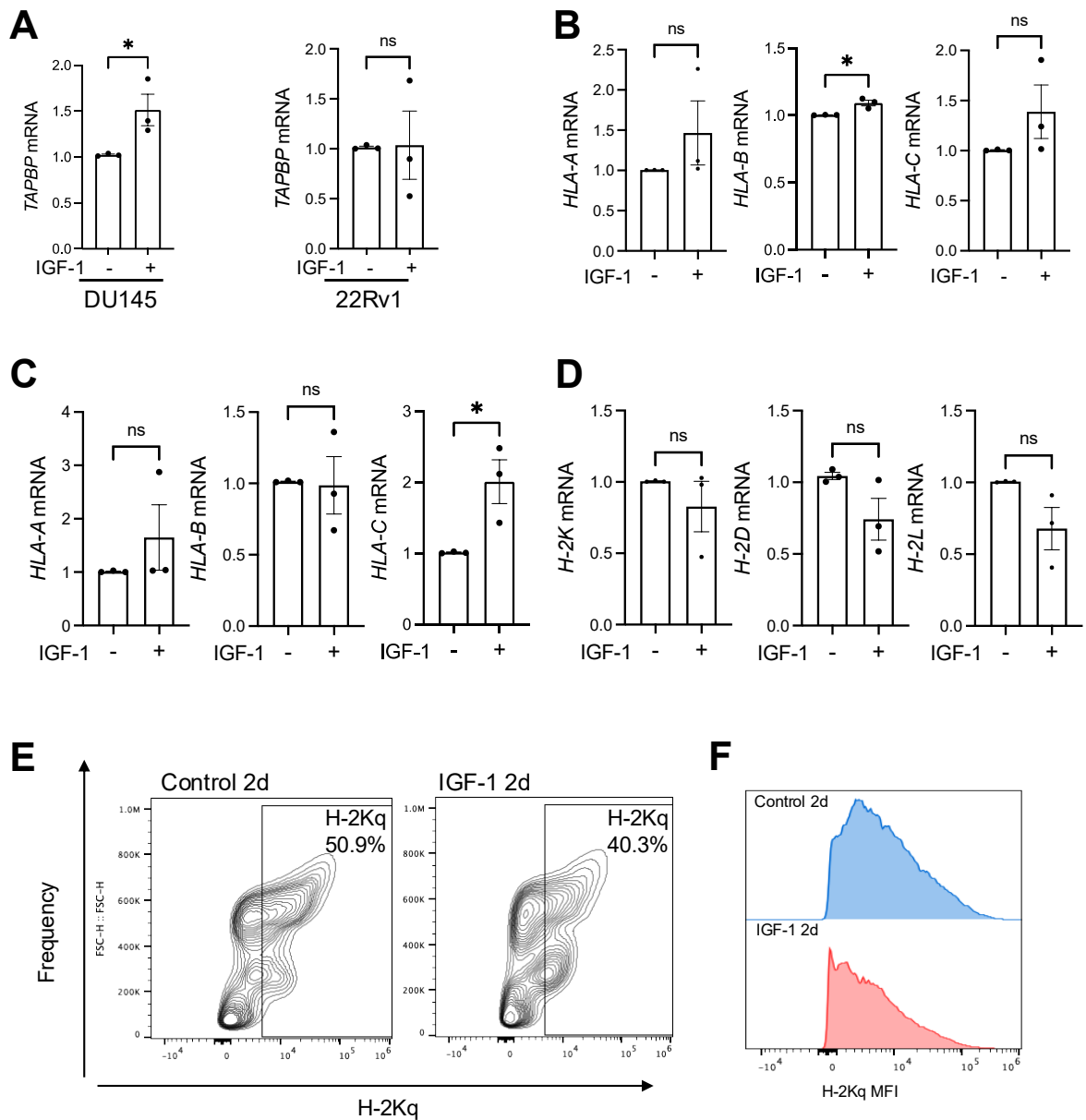
B 22Rv1



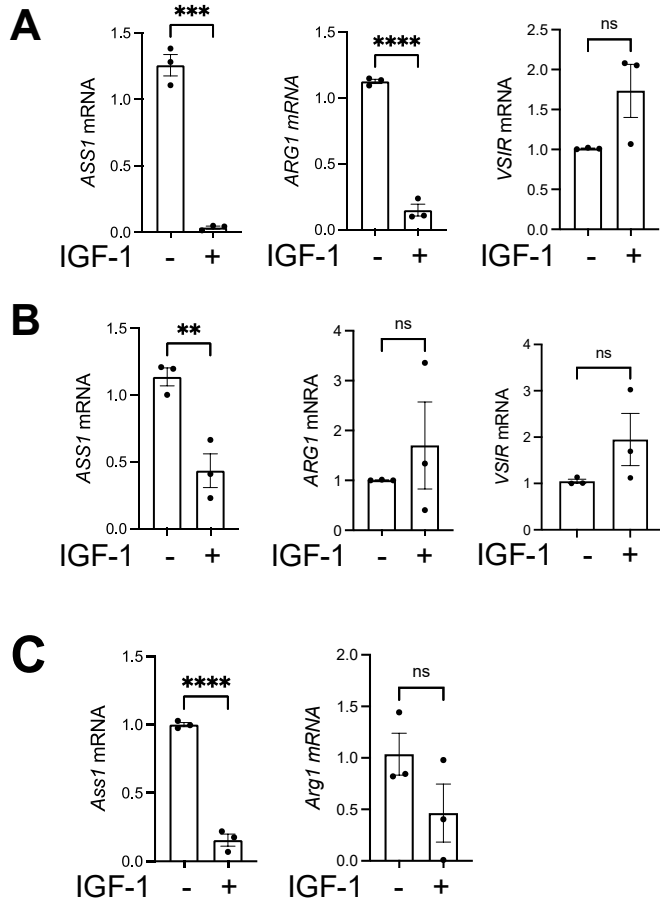
C Myc-CaP



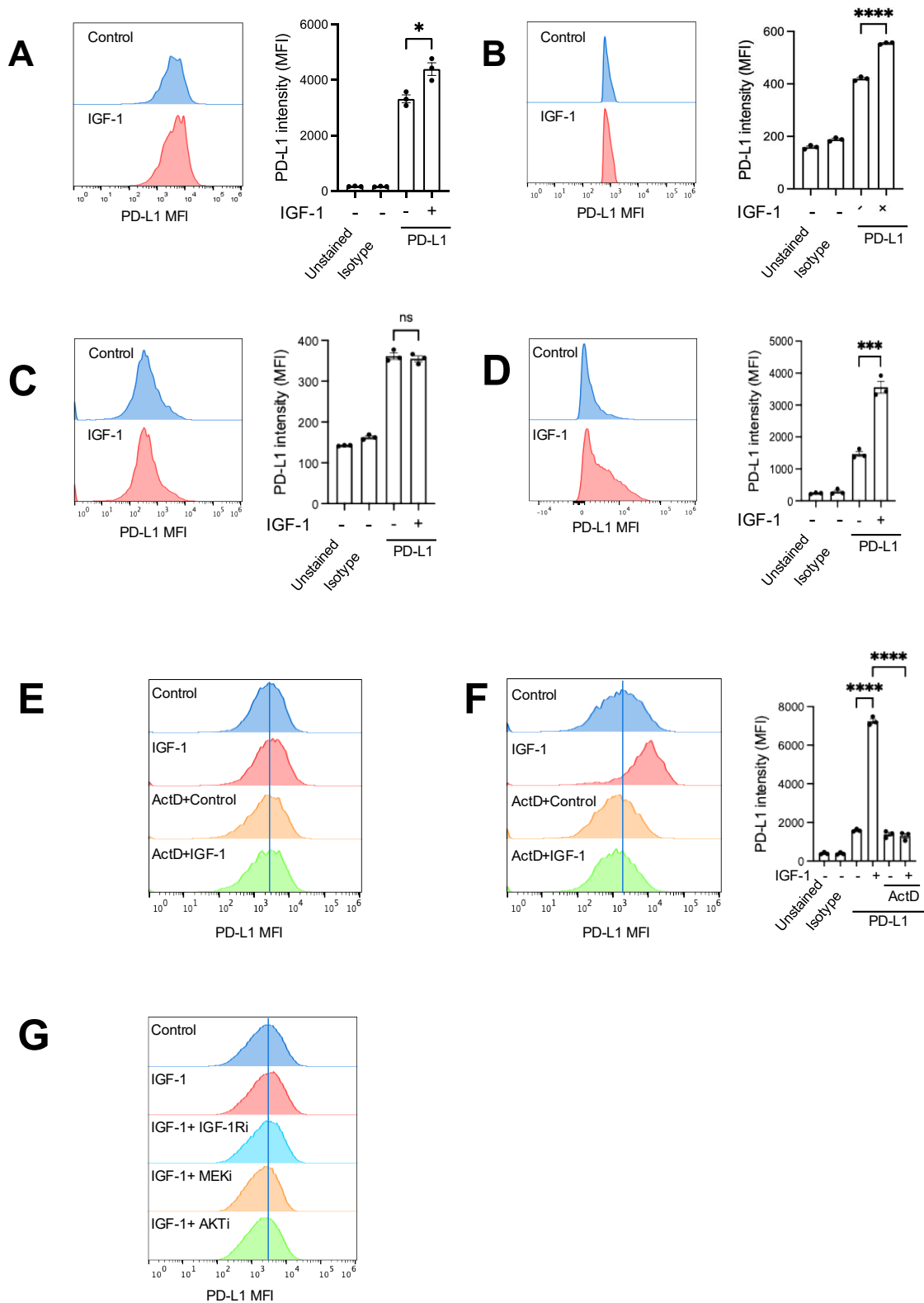
Supplementary Figure S2. IGF-deregulated genes that influence protein degradation. PCa cells **A.** DU145, **B.** 22Rv1 and **C.** Myc-CaP were treated for 24 hr with 30 nM IGF-1 or solvent (control) and tested for expression of the indicated genes by RT-qPCR. Graphs: mean \pm SEM of three independent analyses. * $p < 0.05$; ** $p < 0.01$; *** $p < 0.001$; **** $p < 0.0001$; ns, nonsignificant.



Supplementary Figure S3. IGF-1 does not cause consistent deregulation of Class I genes in human or murine PCa cells. PCa cells were serum starved for 24 hrs and treated with solvent (control) or 30 nM IGF-1. **A**, Effects of IGF-1 on *TAPBP* mRNA expression on left, DU145; right, 22Rv1. **B-D**. Effects of IGF-1 on expression of Class I alleles in: B, DU145; C, 22Rv1; D, Myc-CaP. Graphs represent mean \pm SEM of three independent analyses (* p <0.05; ns, nonsignificant). **E-F**. Representative flow cytometry plots of H2Kq percentage positivity (E) and MFI surface expression (F) in Myc-CaP cells treated with 30 nM IGF-1 or solvent after 2 days.

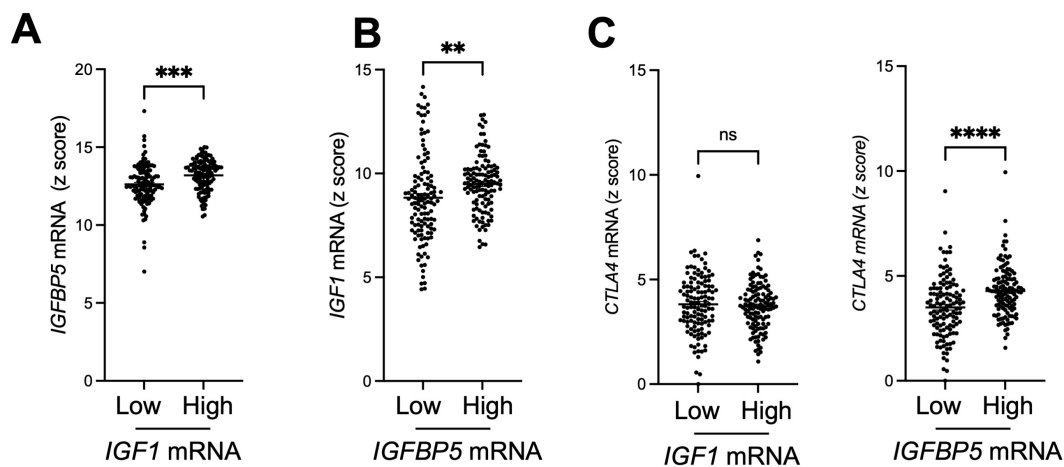


Supplementary Figure S4. Effects of IGF-1 on expression of immune suppressors. Prostate cancer cells were serum starved for 24 hrs and treated with solvent (control) or 30 nM IGF-1. **A-C.** Effects of IGF-1 on *ASS1*, *ARG1* and *VSIR* expression assessed by qRT-PCR in DU145 (A), 22Rv1 (B) and Myc-CaP (C). *Vsir* mRNA expression was undetectable in Myc-CaP. Graphs represent mean \pm SEM (n=3 independent samples. *p< 0.05; **p<0.01; ***, p<0.001; ****, p<0.0001; ns, nonsignificant).

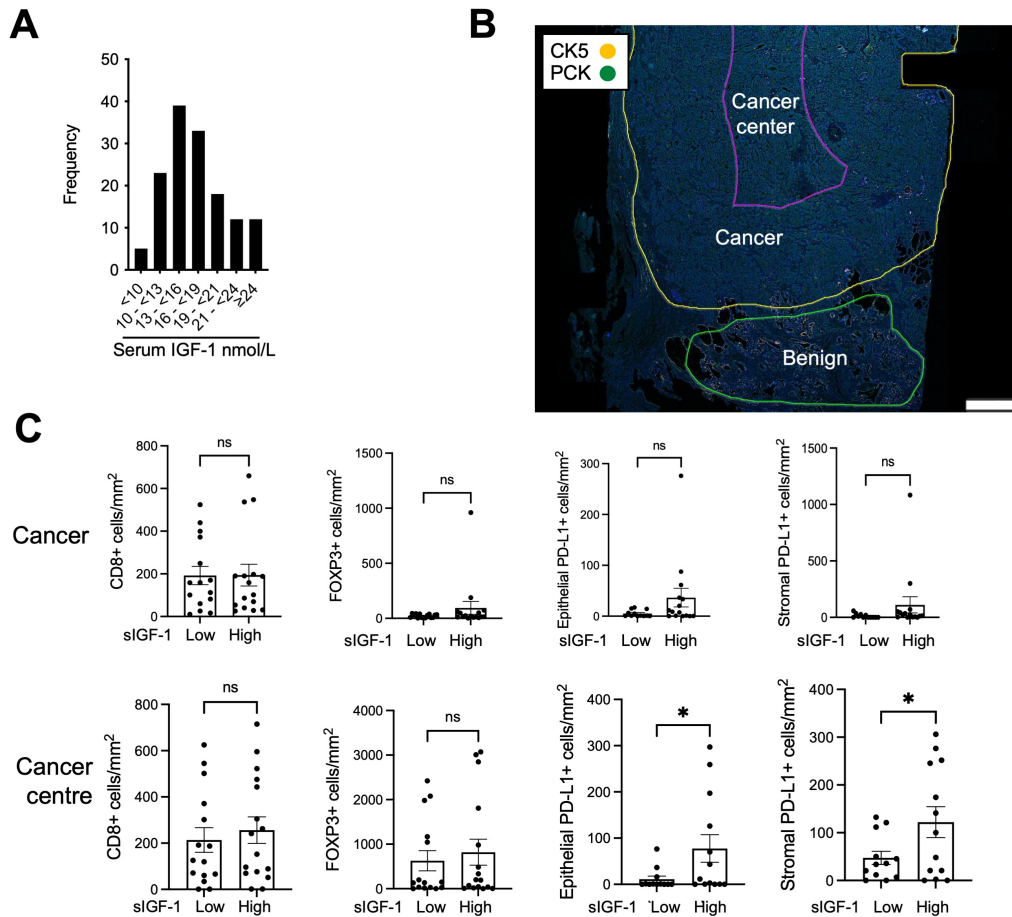


Supplementary Figure S5. Effects of IGF-1 on PD-L1 surface expression. **A.** DU145 cells were treated with 30 nM IGF-1 or solvent (control) in full medium (10% FBS) and PD-L1 surface expression measured using flow cytometry. **B-D.** Cancer cells were serum starved for 24 hrs and treated with solvent (control) or 30 nM IGF-1. Effects of IGF-1 on PD-L1 surface expression was measured using flow cytometry on prostate cancer cell lines Myc-CaP (B) and 22Rv1 (C), and colorectal cancer cell line H747 (D). Left, representative histogram; right, expression

measured as MFI, mean \pm SEM from 3 independent experiments. **E.** Flow cytometry histogram of PD-L1 surface expression in DU145 cells pre-treated with 1 μ g/mL actinomycin D for 2 hours, followed by the addition of 30 nM IGF-1. PD-L1 expression was assessed 24 hours later. Blue vertical line indicates PD-L1 MFI in untreated control cells **F.** H747 cells were treated as in E. and PD-L1 surface expression measured. Left, representative histogram with blue vertical line indicating PD-L1 MFI in untreated control cells; right, expression measured as MFI, mean \pm SEM from 3 independent experiments. **G.** Flow cytometry histogram of PD-L1 surface expression in DU145 cells pre-treated for 1 hour with 300 nM IGF-1R inhibitor BMS-754807, 5 μ M AKT inhibitor AZD5363, or 50 nM MEK inhibitor trametinib, followed by 30 nM IGF-1 stimulation for 24 hours. Blue vertical line indicates PD-L1 MFI in untreated control cells. Graphs represent mean \pm SEM (n=3 independent samples. *p<0.05; **p<0.01; ***, p<0.001; ****, p<0.0001; ns, nonsignificant).



Supplementary Figure S6. Association of IGF axis activation markers with immune checkpoints in clinical prostate cancers. A, B and C, Tumours from TCGA prostate adenocarcinoma (n=498) were divided based on highest and lowest quartiles of tumour endogenous *IGF1* (n= low:124, high=125) and *IGFBP5* (n= low: 124, high =125) mRNA (Z score relative to all samples). A, Association between *IGF1* mRNA and *IGFBP5* mRNA in prostate cancer tissues. B, Association between *IGFBP5* mRNA and *IGF1* mRNA in prostate cancer tissues. C, Association between *IGF1* (left) and *IGFBP5* (right) mRNA and *CTLA4* mRNA expression in prostate cancer tissue. *p<0.05; **p<0.01; ***p<0.001; ****p<0.0001; n.s., nonsignificant.



Supplementary Figure S7. IGF axis activation associates with immune checkpoints and infiltrates in clinical PCa. **A.** Serum IGF in 139 men with localized PCa recruited to ProMPT study. Assay used IDS-iSYS IGF-I assay (Immunodiagnostic Systems). All values were within normal range (7.0-31.7 nmol/L) for males >32 yr [1]. **B.** PCK and CK5 from mIF of radical prostatectomy, marked up for benign, cancer, cancer center. **C.** Quantification of CD8+ T-cells, FOXP3+ Tregs, epithelial and stromal PD-L1+ cells in cancer (upper) and cancer centre (lower) in high vs low serum IGF-1 (sIGF-1) patients. Numbers in FOXP3+, CD8+ analysis: n = 15 low, 16 high sIGF-1 (1 lost due to technical issues); PD-L1+: n = 12 low, 13 high sIGF-1 patients (7 lost).

Supplementary references

1. Bidlingmaier, M. *et al.* Reference intervals for insulin-like growth factor-1 (IGF-I) from birth to senescence: results from a multicenter study using a new automated chemiluminescence IGF-I immunoassay conforming to recent international recommendations. *J Clin Endocrinol Metab* **99**, 1712-1721 (2014).
<https://doi.org/10.1210/jc.2013-3059>